

# Optimal Pressure Sensor Placement and Assessment for Leak Location Using a Relaxed Isolation Index: Application to the Barcelona Water Network<sup>☆</sup>

Miquel À. Cugueró-Escofet, Vicenç Puig, Joseba Quevedo<sup>a</sup>

<sup>a</sup>Supervision, Safety and Automatic Control Research Center (CS2AC), Polytechnic University of Catalonia (UPC), Terrassa Campus, Gaia Research Bldg., Rambla Sant Nebridi, 22. 08222 Terrassa, Barcelona, Spain (e-mail: {miquel.angel.cugueru,vicenc.puig,joseba.quevedo}@upc.edu).

---

## Abstract

Water distribution networks are large complex systems affected by leaks, which often entail high costs and may severely jeopardise the overall water distribution performance. Successful leak location is paramount in order to minimize the impact of these leaks when occurring. Sensor placement is a key issue in the leak location process, since the overall performance and success of this process highly depends on the choice of the sensors gathering data from the network. Common problems when isolating leaks in large scale highly-gridded real water distribution networks include leak mislabelling and the obtention of large number of possible leak locations. This is due to similarity of leak effect in the measurements, which may be caused by topological issues and led to incomplete coverage of the whole network. The sensor placement strategy may minimize these undesired effects by setting the sensor placement optimisation problem with the appropriate assumptions (e.g. geographically cluster alike leak behaviors) and by taking into account real aspects of the practical application, such as the acceptable leak location distance. In this paper, a sensor placement methodology considering these aspects and a general sensor distribution assessment method for leak diagnosis in water distribution systems is presented and exemplified with a small illustrative case study. Finally, the proposed method is applied to two real District Metered Areas (DMAs) located within the Barcelona water distribution network.

© 2017 Published by Elsevier Ltd.

*Keywords:* Sensor placement, fault detection and isolation, leak location, correlation coefficient, water distribution networks.

---

## 1. Introduction

An issue of great concern in water drinking networks is the existence of leaks at the distribution stage, highly related with water resource savings and management costs. The classical approach to leak control is passive, i.e. a leak is repaired when it becomes visible. Recently developed acoustic instruments also allow non-visible leak location [1], but the use of such instrumentation in large-scale water networks is expensive and time-consuming. An acceptable approach is to divide the network into District Metered Areas (DMAs), where the *flow* and the *pressure* are measured [2, 3], and use a leak control-system on a permanent basis. Concretely, leaks affecting DMAs increase the flow and decrease the pressure magnitudes at the DMA inputs. Several empirical studies propose mathematical models to characterise the leak flow magnitude with respect to the pressure magnitude at the leak location point [4, 5].

---

<sup>☆</sup>This work has been partially funded by the Spanish Ministry of Science and Technology through the Project ECOCIS (Ref. DPI2013-48243-C2-1-R) and Project HARCRCIS (Ref. DPI2014-58104-R), and by EFFINET grant FP7-ICT-2012-318556 of the European Commission.

10 Best practice in the analysis of DMA flows consists in estimating the leak magnitude when the flow is minimum.  
11 This typically occurs at night time, when customers' demand is low and hence the leak magnitude over the total  
12 DMA flow is at its highest rate [3]. Therefore, an accepted approach by the practitioners is to monitor the minimum  
13 DMA night flow in order to detect and repair the leaks when occurring, while also employing techniques to estimate  
14 the corresponding leak magnitude [3]. However, the leak detection may not be straightforward, since different kind  
15 of phenomena e.g. unpredictable variations in the customers' demand or measurements' noise, long-term trends or  
16 seasonal effects, may occur.

17 Several works in the literature have addressed the leak location problem in DMAs. In [6], a review of transient-  
18 based leak detection methods is summarized. In the seminal work [7], a model-based leak detection and location is  
19 solved by means of a least-squares estimation problem. However, the latter problem is challenging when considering  
20 the non-linear models involved. Alternatively, a method based on pressure measurements and leak sensitivity analysis  
21 is proposed in [8], where a set of residuals —generated as the difference between pressure measurements provided by  
22 several sensors installed within the DMA and their estimations by the network hydraulic model— is analysed consid-  
23 ering a certain threshold, which takes into account practical factors e.g. the model uncertainty and the measurement  
24 noise. This approach shows satisfactory results under ideal conditions, but its performance degrades when considering  
25 nodal demand uncertainty and measurement noise. This technique is improved in [9], where an extended time horizon  
26 analysis is considered and a comparison of the performance using different metrics is presented.

27 The performance of the leak location approach is highly dependent on the sensor number and placement within  
28 the DMA. Hence, the sensor placement strategy is a key issue to consider in the overall leak location process. There is  
29 an important trade-off between the number of sensors and the subsequent cost preventing the use of a high number of  
30 sensors for leak location purposes. Consequently, this number should be optimised at the sensor placement stage, in  
31 order to produce the maximum benefit i.e. maximize the leak location performance at the minimum cost. According  
32 to these constraints, the sensors considered are pressure sensors since they are a cheaper alternative to flow meters  
33 for the company managing the network. However, the methodology presented here may also be used for alternative  
34 sensor placement setups e.g. combining pressure and flow meters as in [10], or chlorine meters for water quality  
35 fault diagnosis. Hence, the methodology may be arranged with minor modifications to the placement of other type of  
36 sensors.

37 Regarding sensor placement for fault detection and isolation (FDI) purposes, several works concerning this subject  
38 may be found in the literature. Some approaches consider the study of structural matrices in order to locate sensors  
39 based on isolability criteria [11]. In [12], an optimal set of sensors for model-based FDI is sought by means of an  
40 optimisation method based on binary linear programming. These works are embraced in the general framework of FDI  
41 of dynamic systems. However, they are not specially suited to consider the non-explicit non-linear set of equations  
42 describing a water distribution network. Alternatively, several works treated the sensor placement problem when  
43 applied to water distribution networks, most of them addressing the water contamination monitoring (e.g. [13, 14]),  
44 where sensor placement is considered in a large water distribution network in order to detect malicious introduction of  
45 contaminants. Regarding leak location, less contributions addressed the problem of sensor placement. This problem  
46 is studied in [15], where an strategy based on the leak isolability maximization is considered to optimally place the  
47 sensors based on the water network structural model, and in [8], where an optimal sensor placement is formulated  
48 as an integer programming problem, similarly as presented here. Also, an entropy-based approach for efficient water  
49 loss incident detection is introduced in [16].

50 Furthermore, leak location in real water networks involves discrimination among a high number of possible leak  
51 locations —typically, the DMA nodes—, which often leads to mislabel the actual leak location due to the limited  
52 number of sensors available. However, in practical situations there is no need to locate the leak at the exact point where  
53 is produced, since final on-the-ground leak location techniques —e.g. ground-penetrating radar, acoustic listening  
54 devices [17]— may precisely locate them starting from a close area where the actual leak is occurring. Hence,  
55 this calls for a methodology of sensor placement trying to cluster similar leak behaviors geographically, in order to  
56 minimize the number of installed sensors and locate the leak within a certain cluster distance precision.

57 Having this into account, in this paper a new approach for sensor placement focused on leak location in DMAs is  
58 proposed, based on the method introduced in [18]. Alternatively to [8], the approach presented here does not binarize  
59 the sensitivity matrix, but instead use the complete numerical information of this matrix, leading to better leak location  
60 performance as pointed out in [18, 9]. The use of the numerical sensitivity matrix in the sensor placement problem  
61 requires the reformulation of the optimisation problem introduced in [8], since even both approaches are formulated as

an integer optimization problem, isolability conditions considered in the former do not apply here. This reformulation leads to a non-linear integer optimization problem of large dimension that cannot be tackled with deterministic solvers, but with heuristic approaches. Here the use of Genetic Algorithms (GAs) is proposed, since they are a well suited approach to handle problems of this nature [19, 20]. The novel aspects of the sensor placement methodology are, first, to reduce the effect of the leak mislabelling at the sensor placement stage, trying to geographically cluster nodes with similar leak signature. Hence, the sensor distribution favouring this clustering is selected, and the rest are discarded. The second novel aspect of the paper is the proposal of an assessment methodology, using new figures of merit in order to provide the goodness of a certain sensor set from the leak location point of view after the sensors are placed. The assessment indices proposed assume that the leak location algorithm will be based on the correlation between leak signatures, but are independent of the methodology used to place the sensors. Hence, the intrinsic leak mislabelling that may occur in real DMAs with a low ratio between sensors and network nodes is taken into account. To the knowledge of the authors, the use of a general assessment in terms of potential number of isolated leaks is not present in the literature. In [10], an assessment based on the isolation distance is presented in a real DMA, but this do not include the goodness of the sensor distribution regarding the number of isolable leaks for the whole network. The methodology presented is first illustrated in a small example network and then evaluated in several DMAs, located within the Barcelona water network.

The paper is organized as follows: the leak location methodology used as the basis for this work is introduced in Section 2. The sensor placement methodology is presented in Section 3, and the isolability assessment used to evaluate the goodness of the sensor set proposed is introduced in Section 4. The application case studies, based on several DMAs, and the results obtained applying the methodology proposed are shown in Section 5. Finally, in Section 6, some concluding remarks and future work are given.

## 2. Leak Location Problem

The leak location problem may be divided in two different levels: the sensor placement stage and the leak location stage, given a set of sensors. The leak location approach is summarised in this section, since it is the basis of the sensor placement algorithm formulation proposed in this work.

The leak location methodology considered here aims to locate leaks within a DMA by means of some pressure measurements gathered from the network and their estimations, obtained by a network hydraulic model. For a given DMA with  $N$  demand nodes and  $M$  pressure sensors, the leak detection methodology relies on the computation of the residuals  $\mathbf{r} = [r_1 \dots r_M]^T$ , where  $r_i \in \mathbf{r}$  is the difference between the pressure measurement  $p_i$  and its corresponding estimation  $\hat{p}_i$  obtained from a leakless simulation using the corresponding network hydraulic model as follows,

$$r_i = p_i - \hat{p}_i, \quad i = 1, \dots, M, \quad (1)$$

having one residual per each available pressure measurement within the DMA. The number and placement of the sensors is a key issue in the performance of the leak location method and is the target of this paper.

On the other hand, the leak location method relies on the study of the residual vector in (1) by means of sensitivity analysis, aiming to determine the effect of each particular leak on every available pressure sensor measurement at a certain time by means of the sensitivity matrix defined as follows,

$$\mathbf{S} = \begin{pmatrix} s_{11} & \dots & s_{1N} \\ \vdots & \ddots & \vdots \\ s_{M1} & \dots & s_{MN} \end{pmatrix}, \quad (2)$$

considering  $M \leq N$  sensors within the network and  $N$  possible faults (assuming leaks only in nodes) with

$$s_{ij} = \frac{\hat{p}_{ij} - \hat{p}_i}{f_j}, \quad i = 1 \dots M, j = 1 \dots N, \quad (3)$$

where  $\hat{p}_i$  is the leakless scenario pressure estimation in node  $i$  and  $\hat{p}_{ij}$  is the pressure estimation in node  $i$  due to leak  $f_j$  scenario occurring in node  $j$ .

100 To obtain the sensitivity matrix  $\mathbf{S}$ , a leak scenario is generated per each node by numerical simulation, using  
 101 EPANET hydraulic solver [21]. The sensitivity vector corresponding to each column of the sensitivity matrix  $\mathbf{S}$   
 102 is then obtained as follows,

$$\mathbf{s}_j = \begin{bmatrix} s_{1j} \\ \vdots \\ s_{Mj} \end{bmatrix}, \quad j = 1, \dots, N, \quad (4)$$

103 which is also known as leak signature. Each simulated fault scenario is performed by setting a leak of magnitude  $f_j$  in  
 104 the  $j^{\text{th}}$  DMA network node. This procedure is repeated for all the  $N$  existing network nodes. Then, matching both the  
 105 residual vector in (1) and the sensitivity vectors in (4), leak location may be performed by checking which node has  
 106 the highest potential to present a leak. This analysis may be performed by using different metrics [22]. Here, a method  
 107 presented in [18, 10], based on the correlation between residual and sensitivity vectors, is considered. According to  
 108 the study in [9], this method presents the best performance for leak location. However, it should be remarked that the  
 109 sensor placement method presented here could be also applied when considering alternative leak location methods  
 110 using the sensitivity matrix (2).

111 The current metric considered here for leak location is based on the correlation function given by the inner product  
 112 of the regressor vector in (1) and the sensitivity vector in (4), for each particular fault in node  $j$

$$\gamma_j = \frac{\mathbf{s}_j^T \mathbf{r}}{\|\mathbf{s}_j\| \|\mathbf{r}\|}. \quad (5)$$

113 Then, the highest correlation determines the candidate leaky node  $k$ ,

$$\gamma_k = \max(\gamma_1, \dots, \gamma_N). \quad (6)$$

114 The objective here is to develop a methodology to place a given number of sensors,  $M$ , within a DMA in order  
 115 to obtain a sensor set maximizing leak isolability under realistic conditions. In DMAs with a large number of nodes,  
 116 the sensitivity to different leaks occurring in different nodes may be very similar. This sensitivity similarity may  
 117 lead to confusion between different leaks, specially when a low number of sensors is available and uncertainty in the  
 118 measurements and the model is present, which is generally the actual situation. This situation may be solved e.g. by  
 119 increasing the number of sensors, in order to increase the dimension of the leak signature, or by placing the sensors  
 120 with a methodology clustering the nodes presenting sensitivity similarity, as suggested by the methodology presented  
 121 here. This sensor placement methodology, which relies on the leak location scheme presented in this section, is  
 122 introduced in the next section.

### 123 3. Sensor Placement Methodology

#### 124 3.1. Sensor Placement as an Optimisation Problem

125 The goal of this methodology is to place the best sensor set in order to locate the leak as precisely as possible  
 126 within the considered water network. The sensor distribution method is based on the system sensitivity matrix (2). As  
 127 discussed in the introduction, a former methodology is presented in [8], where the residuals and the sensitivity matrix  
 128 are binarized by a certain threshold value. In the approach presented here, the complete numerical information is used  
 129 in order to avoid data loss introduced by the binarization in order to increase leak discriminability [18]. Moreover,  
 130 the sensor placement method presented here uses a relaxed isolation index to better handle some real-world effects  
 131 affecting water network systems, such as system non-linearity, sensor measurements resolution and model uncertainty  
 132 (e.g. in the demands or network element parameters). These real-world effects cause deviation between the modelled  
 133 and the actual system behavior, which may lead to mislabel the latter, and to confuse different leak scenarios —  
 134 sensitivity vectors in (4)—. However, if the confusion involves geographically close behaviors, these undesired effects  
 135 do not severely impact the final leak location result. Hence, the optimal sensor distribution aims to place the sensors  
 136 to geographically cluster leaks with similar signature (4). The method presented uses the information of the complete  
 137 sensitivity matrix (2) —i.e. assuming that all the nodes of the network are measured—, which must be computed  
 138 beforehand by numerical simulation. In order to perform the sensor placement of  $M$  sensors, let us define the binary  
 139 decision vector that represents the selected sensors,

$$\mathbf{x} = \begin{pmatrix} x_1 & \cdots & x_N \end{pmatrix}^T, \quad (7)$$

140 where  $x_i = 1$  if the pressure sensor in node  $i$  is installed and 0 otherwise. Defining

$$\mathbf{X}(\mathbf{x}) = \text{diag}(x_1, \cdots, x_N), \quad (8)$$

141 the sensitivity vectors obtained using the set of selected sensors can be represented as follows,

$$\bar{\mathbf{s}}_j(\mathbf{x}) = \mathbf{X}(\mathbf{x})\mathbf{s}_j, \quad j = 1, \cdots, N, \quad (9)$$

142 where  $\mathbf{s}_j$  is the sensitivity matrix obtained when all the  $N$  sensors are available, i.e.  $M = N$ . Hence, the projection  
143 between two different leak signatures  $i$  and  $j$  for a given subset of sensors  $\mathbf{x}$  is introduced by their inner product as  
144 follows,

$$\gamma_{ij}(\mathbf{x}) = \frac{\bar{\mathbf{s}}_i^T(\mathbf{x})\bar{\mathbf{s}}_j(\mathbf{x})}{|\bar{\mathbf{s}}_i(\mathbf{x})||\bar{\mathbf{s}}_j(\mathbf{x})|} = \frac{\mathbf{s}_i^T \mathbf{X}(\mathbf{x})\mathbf{s}_j}{|\mathbf{X}(\mathbf{x})\mathbf{s}_i||\mathbf{X}(\mathbf{x})\mathbf{s}_j|}, \quad i, j = 1, \cdots, N, \quad (10)$$

145 where  $\bar{\mathbf{s}}_i, \bar{\mathbf{s}}_j$  are vectors corresponding to two different fault signatures (columns) for each class (leak) in the sen-  
146 sitivity matrix (2) and  $\gamma_{ij}$  is a measure of similarity between these two classes. From (10), the projection —or  
147 cross-correlation— matrix may be stated as follows,

$$\Gamma(\mathbf{x}) = \begin{pmatrix} \gamma_{11}(\mathbf{x}) & \cdots & \gamma_{1N}(\mathbf{x}) \\ \vdots & \ddots & \vdots \\ \gamma_{N1}(\mathbf{x}) & \cdots & \gamma_{NN}(\mathbf{x}) \end{pmatrix}, \quad (11)$$

148 containing the projection between all the leak signatures in the sensitivity matrix. For a given sensor configuration,  
149 this matrix presents the degree of similarity of each leak with all the leaks considered in the network. The goal is to  
150 find a sensor configuration such that the largest values are in the diagonal of this matrix, whilst the values close to these  
151 largest values correspond to leaks which are not far geographically. It may be noted that this matrix is symmetric, so  
152  $\Gamma = \Gamma^T$ .

153 In order to evaluate the quality of a sensor allocation setup,  $\rho_{ij}(\mathbf{x})$  is applied to (11) as follows,

$$\rho_{ij}(\mathbf{x}) = \left( \gamma_{ij}(\mathbf{x}) \left( 1 - \frac{d_{ij}}{d_{\max}} \right) \right)^{d_c} + \left( (1 - \gamma_{ij}(\mathbf{x})) \frac{d_{ij}}{d_{\max}} \right)^{d_f}, \quad i, j = 1 \dots N, \quad (12)$$

154 where  $\gamma_{ij}$  is the cross-correlation between leak  $i$  and leak  $j$  signature vectors,  $d_{ij}$  is the topological (pipe) distance  
155 between leaky nodes  $i$  and  $j$ ,  $d_{\max}$  is the maximum pipe distance for the whole network, and  $d_c$  and  $d_f$  are tuning  
156 parameters related with the included high-correlated close leaks cluster and the excluded high-correlated distant leaks  
157 subset, for a given  $i$ - $j$  leak pair, respectively. This particular cost function aims to obtain the best sensor configuration  
158 in order to locate the leaky node as precisely as possible, by promoting sensor setups that geographically group leaks  
159 with similar signature. On the one hand, parameter  $d_c$  is related with the isolation zone —or cluster—, i.e. the  
160 zone where the leaks may be mislabelled. An acceptable value for this perimeter, which is provided by the company  
161 managing the network, is about 200 m in a real DMA. Inside this perimeter, alternative on-the-ground techniques  
162 —e.g. ground penetrating radar— are used for finer isolation. Hence,  $d_c$  is selected accordingly, taking into account  
163 the corresponding DMA  $d_{\max}$ , so the cost function value decreases when the distance between high correlated leaks  
164 is below the selected perimeter. On the other hand, parameter  $d_f$  is related with the exclusion zone, i.e. the zone  
165 where leaks should not be mislabelled with the leaks in the isolation zone. Hence,  $d_f$  is selected such that outside  
166 the isolation zone leak mislabelling is penalized, i.e. the cost function value decreases when the distance between

low correlated leaks is above the selected perimeter. The values of  $d_c$  and  $d_f$  parameters should be selected such that (12) range from zero to one for each  $i$ - $j$  leak pair. These parameters may also be used to adjust the target of the optimisation. The bigger  $d_c$ ,  $d_f$ , the narrower the related zone. Generally  $d_c$  is chosen bigger than  $d_f$ , so the slope of the exclusion term is lower, since the exclusion zone embraces all the nodes in the network outside the isolation perimeter. However, if one wants to get focused on the leak isolation zone,  $d_f$  may be chosen arbitrarily high in order to penalise arbitrarily distant nodes. Considering (12), the sensor placement may be stated as an optimisation problem as follows,

$$\begin{aligned} & \underset{\mathbf{x}}{\text{minimize}} && \rho(\mathbf{x}) \\ & \text{subject to} && \sum_{i=1}^N x_i = M, \end{aligned} \quad (13)$$

where

$$\rho(\mathbf{x}) = 1 - \frac{1}{N^2} \sum_{i=1}^N \sum_{j=1}^N \rho_{ij}(\mathbf{x}) \quad (14)$$

is to be optimised over the full  $N$  sensors set available, and  $M$  is a predefined restriction on the number of sensors to install. The cost function in (14) for a single  $i$ - $j$  leak pair is depicted in Figure 1 for illustrative purposes. The criterion to select the parameters  $d_c$  and  $d_f$  may be illustrated with Figure 1b, for a DMA with  $d_{\max} = 1000$  m. Parameter  $d_c$  is selected so  $\gamma_{ij}$  starts decreasing at a normalised distance  $d_{ij}/d_{\max} = 0.2$ , corresponding to a distance of 200 m. Similar criterion is applied for the selection of  $d_f$ , related with the leak exclusion area. Hence, the use of this cost function aims to achieve a sensor distribution obtaining high-correlation/low-distance (first term in (12)) and low-correlation/high-distance (second term in (12)) leak scenario combinations.

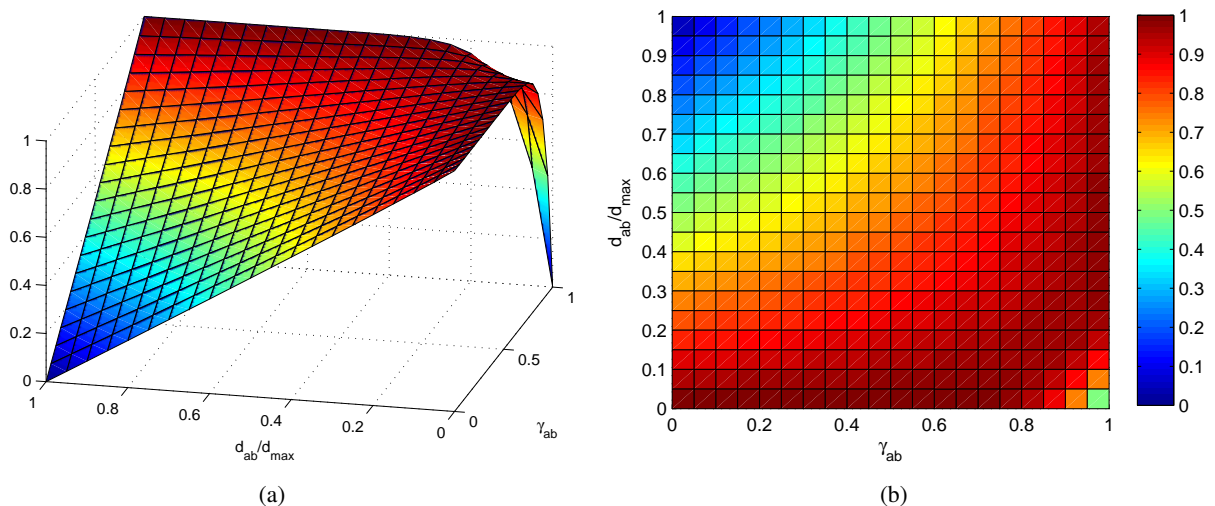


Figure 1: Cost function for a single  $i - j$  pair

The sensor placement optimisation problem (13) is solved using GA, which is a suitable approach for large-scale binary non-linear problems as the one considered here [23]. Further details on the GA parameters utilised to solve this particular problem are given in Section 5.2.

### 3.2. Methodology summary

Considering the optimisation problem presented in Section 3.1, a summary of the methodology for illustrative purposes is presented in Algorithm 1, which states how this methodology should be implemented. As previously

188 mentioned in Section 3.1, it may be noted that the sensitivity matrix (2) must be computed beforehand by numerical  
 189 simulation of the network considered.

---

#### Algorithm 1 Sensor Placement Methodology

---

**Require:**  $S, d_c, d_f, d_{max}, N, M$

Initialise  $\mathbf{x}$ ; {Assign binary random elements to decision vector  $\mathbf{x}$  for  $M$  sensors and  $N$  nodes}

**while**  $\rho(\mathbf{x})$  is not minimum **do**

Obtain  $\mathbf{x}$  for  $M$  sensors; {Optimisation algorithm computes a new potential decision vector}

**for all**  $N^2$   $i$ - $j$  node pairs **do**

Compute  $\gamma_{ij}(\mathbf{x})$ ; {Corresponding projection for  $i$ - $j$  pair is obtained}

Compute  $\rho_{ij}(\mathbf{x})$ ; {Corresponding quality sensor allocation measure for  $i$ - $j$  pair is obtained}

**end for**

Compute  $\rho(\mathbf{x})$ ; {Corresponding cost value is obtained}

**end while**

**return**  $\mathbf{x}$  {Return selected decision vector i.e. optimal sensor set}

---

#### 190 4. Leak Isolability Assessment

191 In order to assess the leak isolability of a given sensor configuration, a metric based on the confusion matrix  
 192 is proposed [24]. Each column of this matrix represents the actual leak, whilst each row stands for the degree of  
 193 similarity with the signature vectors of each considered leak,

$$C = \begin{pmatrix} \kappa_{11} & \cdots & \kappa_{1N} \\ \vdots & \ddots & \vdots \\ \kappa_{N1} & \cdots & \kappa_{NN} \end{pmatrix}, \quad (15)$$

194 where  $\kappa_{ij} \in \{0, 1\}$  for  $i, j = 1 \dots N$ . The name stems from the fact that this representation allows to check a given  
 195 sensor configuration, commonly by the number of correct and incorrect predictions achieved by the leak location  
 196 method compared with the actual leak occurring in the test data. The values of  $\kappa_{ij}$  depend on each particular isolation  
 197 criterion used. Here, a criterion based on the cross-correlation (11) is used to obtain the maximum correlation for each  
 198 actual fault,

$$\gamma_{ij_{max}} = \max_{j \in 1 \dots N} \gamma_{ij}, \quad i = 1 \dots N, \quad (16)$$

199 where  $\kappa_{ij}$  is determined as follows,

$$\kappa_{ij} = \begin{cases} 1 & \gamma_{ij} = \gamma_{ij_{max}} \\ 0 & \text{otherwise} \end{cases}, \quad i, j = 1 \dots N. \quad (17)$$

200 In order to provide less conservative leak isolation results, while still realistic and well suited to the optimisation  
 201 criterion stated in (13), the matrix of pipe distances among nodes of the network are considered,

$$D = \begin{pmatrix} d_{11} & \cdots & d_{1N} \\ \vdots & \ddots & \vdots \\ d_{N1} & \cdots & d_{NN} \end{pmatrix}, \quad (18)$$

202 and the isolation condition (17) may be relaxed by a certain fault isolation cluster distance  $d_{cluster}$  as follows,

$$\kappa_{ij} = \begin{cases} 1 & \max \mathbf{d}_{ij_{max}} < d_{cluster} \quad \text{and} \quad d_{ij} < \max \mathbf{d}_{ij_{max}}, \quad i, j = 1 \dots N, \\ 0 & \text{otherwise} \end{cases} \quad (19)$$

203 where  $\mathbf{d}_{ij_{\max}}$  is the distance between the actual leaky node  $i$  and the node (or nodes) with highest correlation  $\gamma_{ij_{\max}}$   
 204 —i.e. predicted leaky nodes—, and  $d_{\text{cluster}}$  is the maximum allowed distance between the actual leaky node  $i$  and the  
 205 predicted leaky nodes, in order to consider that the leak in  $i$  is correctly isolated. When several predicted faulty nodes  
 206 are obtained, the worst case —i.e.  $\max \mathbf{d}_{ij_{\max}}$ — is considered.

207 The number of correctly isolated leaks is given by the following isolation index,

$$\zeta = \text{tr}(C), \quad (20)$$

208 so the correct isolated faults are those which are assigned to its own class and not to any other possible leak occurring  
 209 in the network. The best isolation index ( $\zeta_{\text{best}}$ ) for a given  $d_{\text{cluster}}$  is obtained when sensors in all nodes are available  
 210 i.e. when  $M = N$ , which states a topological limit,

$$0 \leq \zeta_{\text{opt}} \leq \zeta_{\text{best}} \leq N, \quad (21)$$

211 where  $\zeta_{\text{opt}}$  is the isolation index obtained with the corresponding optimal sensor placement, for a given  $d_{\text{cluster}}$ . Let  
 212 us also define a particular  $\zeta_{\text{opt}}$  and  $\zeta_{\text{best}}$  considering (17), i.e.  $\zeta_{\text{opt}_0}$  and  $\zeta_{\text{best}_0}$ , respectively. Then, a more general  
 213 topological limit which does not depend on the distance between nodes may be given by

$$0 \leq \text{rank } \mathbf{S} \leq \zeta_{\text{opt}_0} \leq \zeta_{\text{best}_0} \leq N, \quad (22)$$

214 where  $\mathbf{S}$  is the sensitivity matrix obtained when all the  $N$  sensors are available, i.e.  $M = N$ . Previous relation is  
 215 meaningful since  $\zeta_{\text{best}_0}$  computation may be infeasible for DMAs with a high number of nodes  $N$ . Then,  $\text{rank } \mathbf{S}$  may  
 216 provide a useful computationally efficient approximation, specially when this magnitude is close to the DMA number  
 217 of nodes  $N$ . It must be noted that, since matrix  $\mathbf{S}$  is affected by the pressure sensor resolution, confusion between  
 218 leaks may be induced (e.g. linear dependency between columns of  $\mathbf{S}$ ) as the DMA size increases.

219 It may also be noted that the ratio  $\phi_{\text{best}} = \frac{\zeta_{\text{best}}}{\zeta_{\text{best}_0}} \geq 1$  suggests the benefit obtained by the geographic relaxation when  
 220 all the sensors are available (the bigger the better), whilst the ratio  $\phi_{\text{opt}} = \frac{\zeta_{\text{opt}}}{\zeta_{\text{opt}_0}} \geq 1$  suggests the geographical relaxation  
 221 benefit for the sensor subset considered. This benefit may be also obtained from an extra coverage percentage over  
 222  $\zeta_{\text{best}}$  as follows,

$$\delta = \frac{\zeta_{\text{opt}} - \zeta_{\text{opt}_0}}{\zeta_{\text{best}}} 100, \quad (23)$$

223 where  $\delta$  is the percentage of extra coverage over  $\zeta_{\text{best}}$ , obtained when geographically relaxing the assessment.

224 A summary of the isolability assessment presented in this section is introduced in Algorithm 2, which states how  
 225 the sensor placement assessment indices may be evaluated in order to evaluate the quality of the solution obtained.

## 226 5. Application Examples: Hanoi and Barcelona Drinking Water Networks

### 227 5.1. Description

228 Several DMAs of different level of complexity are used here in order to show the performance of the sensor  
 229 placement method presented. First, a small DMA is considered to illustrate the method in detail. The Hanoi DMA, an  
 230 existing benchmark network widely used in the literature (see, e.g. [25]), is considered for this purpose (Figure 2). This  
 231 DMA has 31 nodes and 34 links, and delivers water to the end consumers by means of a single input point. Also, two  
 232 different DMAs located in the Barcelona area, with higher nodal density, are used as case studies (Figure 3). On the  
 233 one hand, the *Canyars* DMA (Figure 4) is located at the pressure level 80 within the Barcelona water supply network.  
 234 This DMA has 694 nodes and 719 links, and delivers water to the end consumers by means of a single input point.  
 235 On the other hand, the *Castelldefels Platja* DMA (Figure 5) is located at the pressure level 50 within the Barcelona  
 236 water supply network. This DMA has 4952 nodes and 5116 links, and covers an area of 606 ha. The DMA has two



---

**Algorithm 2** Leak Isolability Assessment
 

---

**Require:**  $D, \mathbf{x}, \Gamma(\mathbf{x}), d_{\text{cluster}}, d_{\text{max}}, N$ 
**for all**  $N^2$   $i$ - $j$  node pairs **do**

 Obtain  $\gamma_{ij_{\text{max}}}$ ; {Maximum correlation for each leak considering the projection for  $i$ - $j$  pairs}

 Obtain  $\mathbf{d}_{ij_{\text{max}}}$ ; {Distance between faulty node  $i$  and node/s with highest correlation  $\gamma_{ij_{\text{max}}}$ }

**if**  $\max \mathbf{d}_{ij_{\text{max}}} < d_{\text{cluster}}$  **and**  $d_{ij} < \max \mathbf{d}_{ij_{\text{max}}}$  **then**
 $\kappa_{ij} = 1$ ; {Leak mislabeling between nodes  $i$  and  $j$ }

**else**
 $\kappa_{ij} = 0$ ; {No leak mislabeling between nodes  $i$  and  $j$ }

**end if**
**end for**

 Compute  $\zeta_{\text{opt}}$ ; {# of correct isolated faults for the optimal sensor set}

 Compute  $\zeta_{\text{best}}$ ; {# of correct isolated faults when  $M = N$ }

 Compute  $\zeta_{\text{opt}_0}$ ; {# of correct isolated faults for optimal sensor set without geographic relaxation}

 Compute rank  $\mathbf{S}$ ; {# of correct isolated faults for sensors in all nodes without geographic relaxation}

 Compute  $\zeta_{\text{best}_0}$ ; {Obtain the rank of the sensitivity matrix}

 Compute  $\phi_{\text{best}}$ ; {Obtain geographic relaxation benefit index when  $M = N$ }

 Compute  $\phi_{\text{opt}}$ ; {Obtain geographic relaxation benefit index for the optimal sensor set}

 Compute  $\delta$ ; {Obtain extra coverage over  $\zeta_{\text{best}}$  when geographically relaxing the isolation}

**return**  $\zeta_{\text{opt}}, \zeta_{\text{best}}, \zeta_{\text{opt}_0}, \text{rank } \mathbf{S}, \zeta_{\text{best}_0}, \phi_{\text{best}}, \phi_{\text{opt}}, \delta, \zeta_{\text{best}}$  {Return assessment indices}
 

---

237 inputs —named Ferrocarril and Pi Tort, respectively— delivering water to the end consumers. The current DMA size  
 238 motivated its reduction to an equivalent hydraulic model of 2828 nodes using skeletonization techniques [26], more  
 239 suitable for high demanding computation algorithms used here.

240 As mentioned in Section 3.2, the first step consists in obtaining the sensitivity matrix (2) by numerical simulation  
 241 of the network under study, i.e. simulating a leak in each node of this network. These scenarios have been generated  
 242 using EPANET hydraulic simulation software, as introduced in Section 2. In order to simulate these DMAs isolated  
 243 from the water supply network, the boundary conditions —i.e. pressure and flow measurements from the network—  
 244 are fixed. Generally, pressure is fixed using a reservoir, and the overall demand is obtained as the sum of the inflow  
 245 distributed through the DMA using a demand pattern model. The total inflow is distributed using a constant coefficient  
 246 —named base demand— in each consumption node. Hence, all the consumptions are assumed to share the same  
 247 profile, whilst the billing information is used to determine the base demand of each particular consumption. A good  
 248 estimation of the demand model is paramount for the real case application.

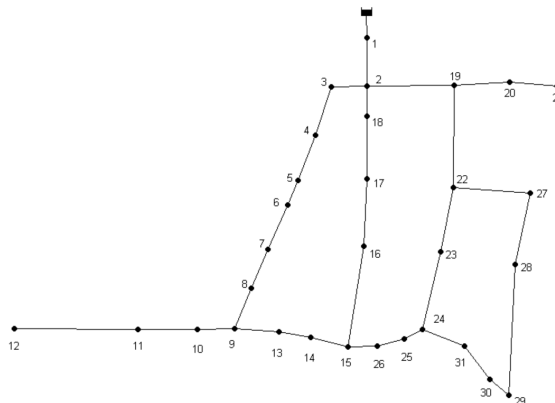


Figure 2: Hanoi DMA

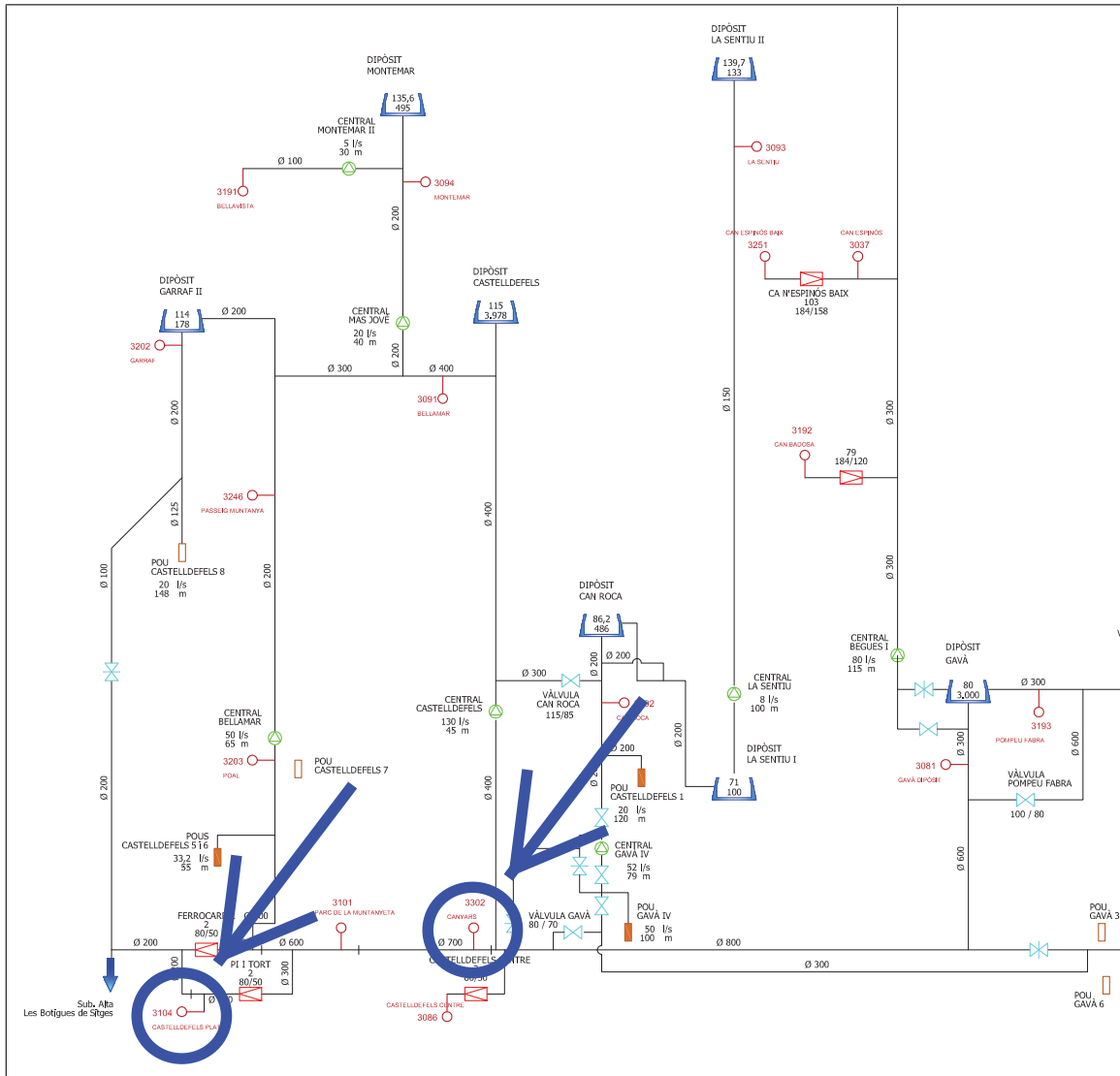


Figure 3: Barcelona Drinking Water Supply Network detail (arrows: Castelldefels Platja and Canyars DMAs, respectively)

## 249 5.2. Results

250 In this section, the results achieved applying the sensor placement methodology described in Section 3 are pre-  
 251 sented. The sensors considered here are pressure sensors, which may be installed in any node of the network. The  
 252 maximum isolation distance  $d_{\text{cluster}}$ , which is a parameter given by the company managing the network, is equal to  
 253 200 m for the Hanoi and Castelldefels DMAs, whilst is assumed of 2000 m for the illustrative Hanoi DMA, due to its  
 254 particularly low nodal density (see Section 4 for a more detailed discussion). For distances below  $d_{\text{cluster}}$ , alternative  
 255 more precise methods are more convenient in order to isolate the leak e.g. ground penetrating radar.

256 To solve the optimization problem (14), GAs available in the global optimization toolbox of MATLAB are used.  
 257 Regarding GA parameters, an initial population of 100 random sensor sets, including the potential sensors to be used,  
 258 is employed to seed the GA algorithm. At this stage, already installed DMA sensors may be included to seed the GA.  
 259 The number of individuals in each generation is set to 100, the maximum number of generations allowed is set to 30,

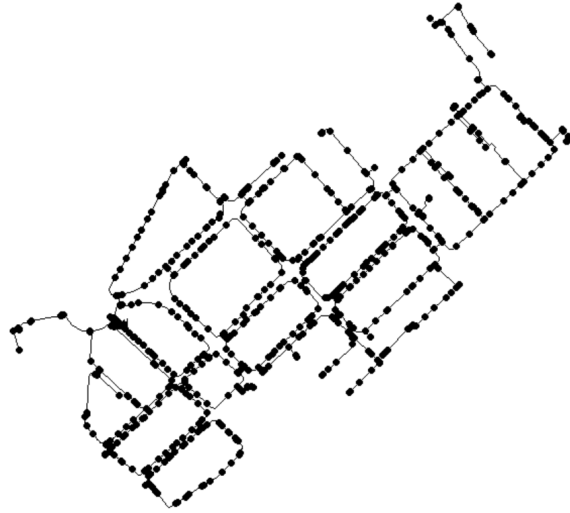


Figure 4: Canyars DMA



Figure 5: Castelldefels Platja DMA

260 the termination tolerance on the fitness function value is set to  $1 \times 10^{-6}$  and the number of generations over which  
 261 cumulative change in fitness function value is less than the termination tolerance —i.e. stall generations limit— is  
 262 set to eight. Since the optimum obtained by the GA is not global, consecutive GA optimisations are conducted until  
 263 fitness function value do not improve between two overall optimisations, aiming to achieve the best possible solution.  
 264 The selection of these parameters takes into account that the optimisation is dealing with real high dimension DMAs  
 265 and the problem may be computationally intensive. In order to face such computational issues, the use of local parallel  
 266 computing is used when multiple labs are available in the host PC, in order to increase computation power. The host  
 267 PC implemented Intel® Core™ i7 Quad-Core processors and 8 GB of 1600 MHz Dual Channel DDR3 memory,  
 268 which allowed the use of such technique.

#### 269 5.2.1. Hanoi DMA

270 The sensor placement results obtained considering Hanoi DMA (Figure 2) are depicted in Figures 7a to 7d. The  
 271 sensitivity matrix  $\mathbf{S}$  is obtained for a 24 h scenario using an emitter coefficient —i.e. discharge coefficient for emitter  
 272 placed at junction, representing the flow in liters per second (LPS) occurring at a pressure drop of 1 psi [21]— of  
 273 5 LPS/psi<sup>0.5</sup>. The sensitivity  $\mathbf{S}$  is concatenated for the 24 hours available, leading to a dimension of  $744 \times 31$ . The

Table 1: Isolation assessment results, Hanoi DMA

Number of sensors	2	3	4	5
$\zeta_{opt}$	14	20	22	22
% of $N$	45	64.5	70.97	70.97
% of $\zeta_{best}$	50	71.43	78.57	78.57
% of $\zeta_{best0}$	45	64.52	70.96	70.96
$\zeta_{opt0}$	30	31	31	31
$\rho$	0.6804	0.6586	0.6445	0.6426

distance used here is the topological distance among nodes, i.e. minimum pipe distance between these elements. This network has a low density of nodes per squared meter, being the minimum distance among the closest nodes of 484 m. Hence,  $d_{cluster}$  should be increased in comparison to a regular network, in order to provide realistic results. For this particular network, the maximum number of isolable faults considering all the sensors available ( $\zeta_{best0}$ ) is 31, and the maximum number of isolable faults considering all the sensors available and  $d_{cluster} = 2000$  m ( $\zeta_{best}$ ) is 28 (90 % of  $N = 31$  nodes forming the network), respectively. According to the specified  $d_{cluster}$  and  $d_{max} = 16426$  m, the cost function parameters have been chosen of  $d_c = 5.36$  and  $d_f = 0.57$ . The evolution of the GA optimisation for each sensor distribution is depicted in Figures 6a to 6d. In the lower row, the latter figures show the evolution of the average distance between individuals among generations in the bottom-left subplot, and the fitness of each individual in the last generation in the bottom-right subplot. In the upper row, the evolution of the best and mean fitness value per generation is depicted in the upper-left subplot, and the GA stopping criteria is depicted in the upper-right subplot. These include the generations limit (set at 30), i.e. the maximum number of generations per optimisation, the time limit (unspecified), i.e. the maximum time in seconds whilst the GA runs before stopping, the stall generations limit (eight), i.e. the number of maximum consecutive generations without improving the average relative change in the best fitness function, over a given function tolerance ( $1 \times 10^{-6}$ ), and the stall time limit (unspecified), i.e. the time interval in seconds after the GA stops if no improvement is obtained in the best fitness value. Time constraints have not been specified since they were not critical parameters in the optimisation. As it is shown in the Figures 6a to 6d, the stopping criteria met in all the optimisations for this particular case is the stall generation limit. Isolation assessment results concerning sensor distribution for different number of sensors (from two to five) are detailed in Table 1. It may be observed how the results obtained between four and five sensors do not improve in terms of  $\zeta_{opt}$ , even a better  $\rho$  is achieved for five sensors at the optimisation stage. In this case, the benefit of installing extra sensors may obtain reduced isolation clusters, but still bigger than  $d_{cluster}$ . Hence, the optimal sensor distribution is obtained for four sensors (Figure 7c) since is the one achieving best  $\zeta_{opt}$  with the minimum number of sensors. For the particular layout of this DMA, which is geographically large ( $d_{max} = 16426$  m) but has low nodal density ( $N = 31$  nodes, with minimum distance among closest nodes of 484 m), the geographical relaxation is not providing any particular benefit ( $\delta$  is negative for all the distributions considered). However, the methodology presented here is useful when leak signature confusion is present, which is not the case in this network ( $\zeta_{opt} = N$  for almost all the sensor distributions considered). Hence, a network of this characteristics is useful for illustrative purposes, but it is not a target network for the proposed methodology, more intended to be used in larger DMAs found in real water networks, as the ones presented in the following sections.

### 5.2.2. Canyars DMA

The sensor placement results obtained when considering Canyars DMA (Figure 4) are depicted in Figures 8a to 8c. The sensitivity matrix  $\mathbf{S}$  is obtained for a fixed leak of 6 LPS, in an hourly sampled scenario comprised between 24/02/2014 9h and 25/02/2014 9h. Thus, the sensitivity  $\mathbf{S}$  is concatenated for the 24 hours available, leading to a dimension of  $16656 \times 694$ . Also, the information in this matrix considers sensor resolution of 0.1 m in order to take into account current technological constraints of the available pressure sensors in the simulated scenario. The distance used here is the topological distance among nodes, i.e. minimum pipe distance between these elements. For this particular network, the maximum number of isolable faults considering all the sensors available ( $\zeta_{best0}$ ) is 399, and the maximum number of isolable faults considering all the sensors available and  $d_{cluster} = 200$  m ( $\zeta_{best}$ ) is 398 (57 % of  $N = 694$  nodes forming the network). According to the specified  $d_{cluster} = 200$  m and  $d_{max} = 888$  m, the cost function

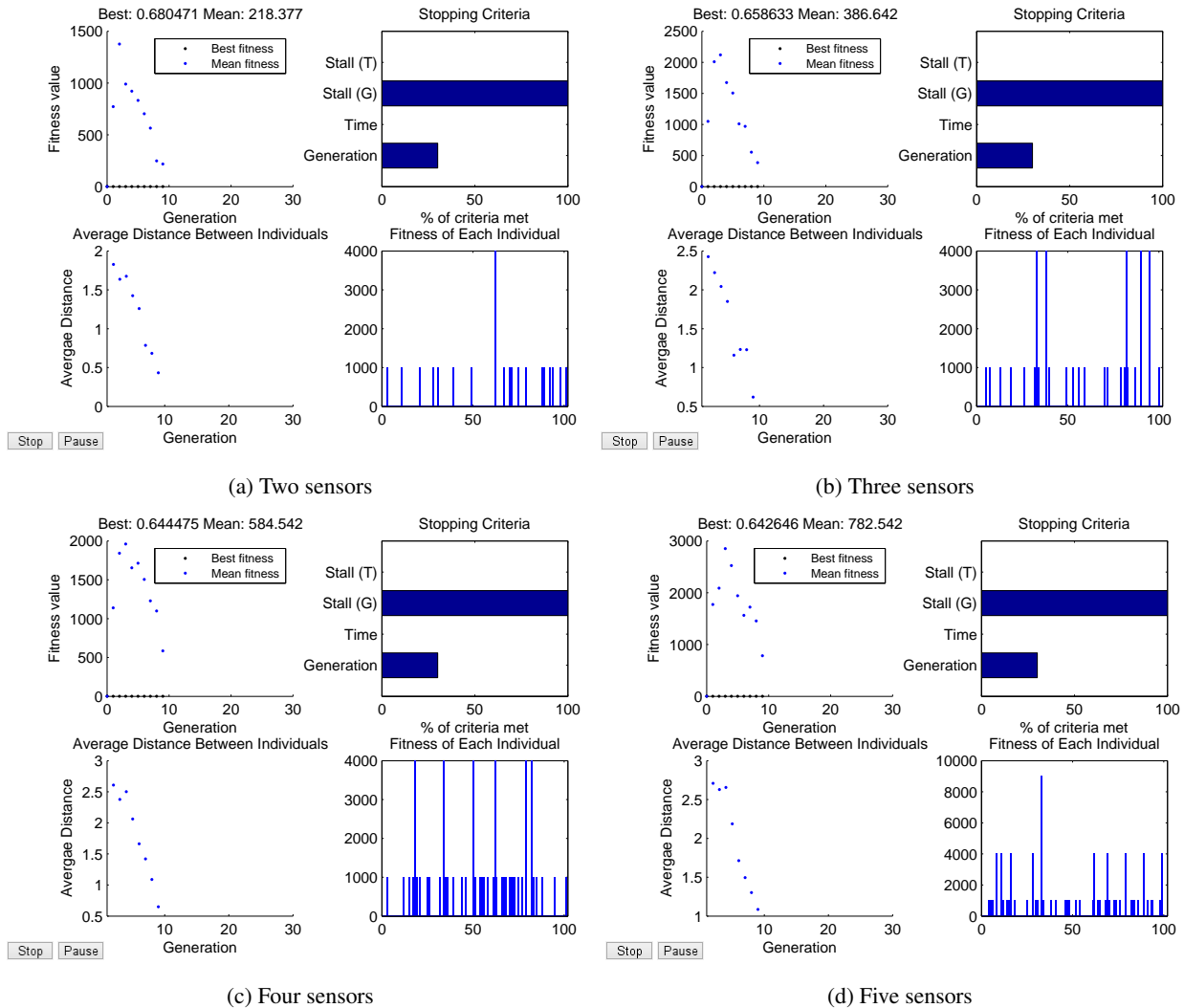


Figure 6: Genetic Algorithms optimisation evolution in Hanoi DMA

314 parameters have been chosen of  $d_c = 8.31$  and  $d_f = 1.04$ , respectively.

315 Leak isolation assessment results concerning sensor distribution for different number of sensors (from two to four)  
 316 are detailed in Table 2. It may be observed how the relaxation by  $d_{cluster}$  does not have much effect when having all the  
 317 sensors available (i.e.  $\phi_{best} \approx 1$ ), but it does for a limited sensor set (see Table 2) e.g. for two sensors, with  $\zeta_{opt} = 267$   
 318 and  $\zeta_{opt_0} = 116$ ,  $\delta = 38\%$  extra coverage over  $\zeta_{best}$  is achieved when geographically relaxing the assessment. It may  
 319 also be observed how the results obtained between three and four sensors do not improve in terms of  $\zeta_{opt}$ , even a better  
 320  $\rho$  is achieved for four sensors at the optimisation stage. In this case, the benefit of installing extra sensors may obtain  
 321 reduced isolation clusters, but still bigger than  $d_{cluster}$ . Hence, since the coverage of the network is high (97% of  $\zeta_{best}$ ),  
 322 the optimal sensor distribution is obtained for three sensors (Figure 8b), since is the one achieving best  $\zeta_{opt}$  with the  
 323 minimum number of sensors.

324 The impact of sensors resolution is also worth to be noted. Although it does not have impact on the maximum  
 325 number of isolable faults  $\zeta_{best} = 398$ —hence, the maximum achievable coverage is not limited by the sensors resolu-  
 326 tion but by the topological network setup, when sufficient number of sensors are available—, it does have impact on  
 327  $\zeta_{opt}$  for different sensor setups—hence, for limited information gathered from the network, sensor resolution effect is  
 328 noticeable—. For example, considering five full-resolution sensors setup, almost complete coverage of the network

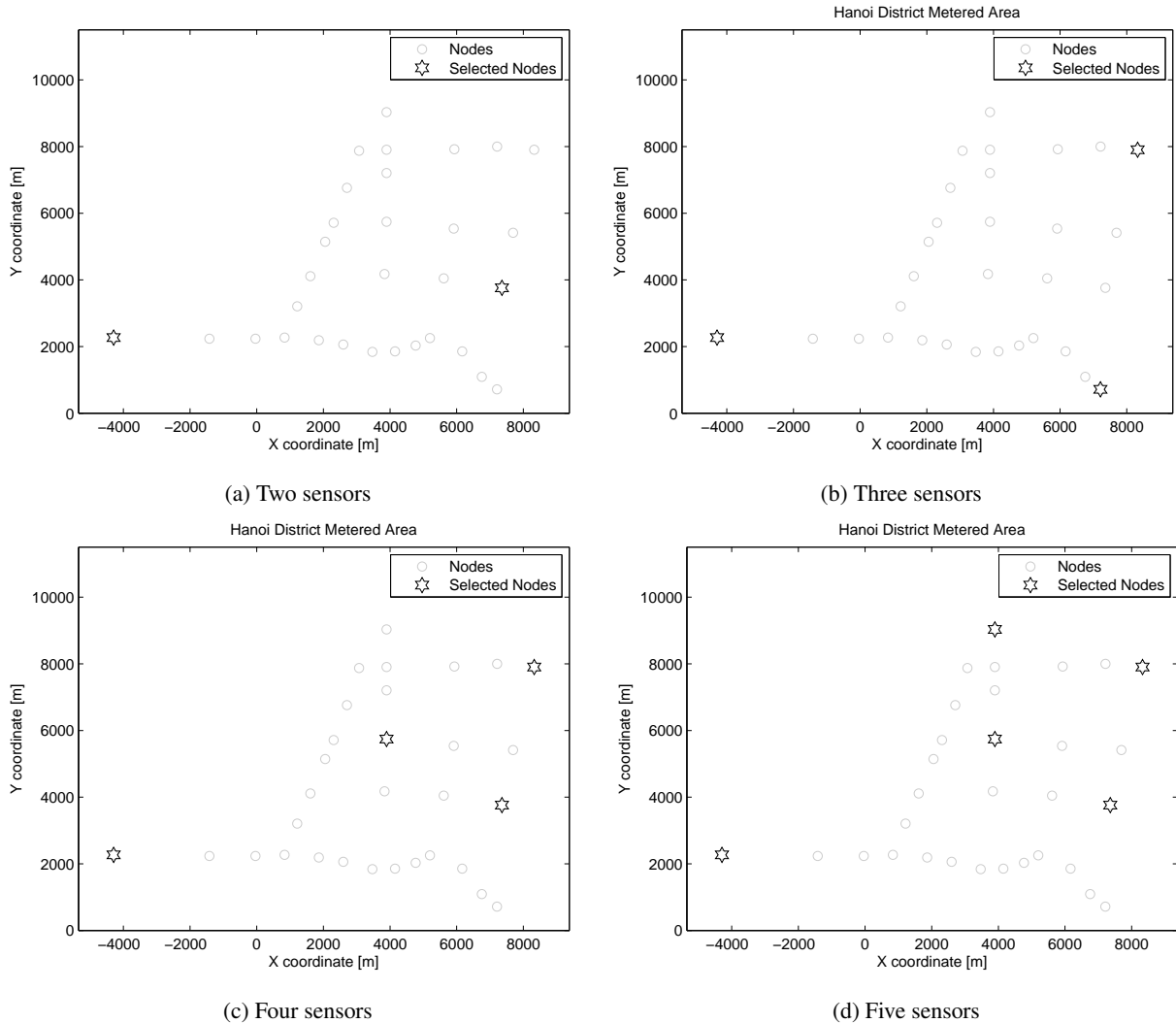


Figure 7: Sensor placement in Hanoi DMA

329 is achieved ( $\zeta_{\text{opt}} = 395$ ), against the 388 isolable faults achieved by the five limited-resolution (0.1 m) sensors setup  
 330 counterpart.

### 331 5.2.3. Castelldefels Platja DMA

332 The sensor placement results obtained considering *Castelldefels Platja* network (Figure 4) are depicted in Fig-  
 333 ures 9a to 9c. The sensitivity matrix  $\mathbf{S}$  is obtained for an emitter coefficient of  $0.92 \text{ LPS/psi}^{0.5}$ , in an hourly sampled  
 334 scenario comprised between 24/02/2014 9h and 25/02/2014 9h, so  $\mathbf{S}$  is concatenated for the 24 hours available and is  
 335 of dimension  $67872 \times 2828$ . Also, the information in this matrix is truncated by sensor resolution (i.e. 0.1 m). The  
 336 distance used here is the topological distance among nodes, i.e. minimum pipe distance between these elements. For  
 337 this particular network, the computation of  $\zeta_{\text{best}_0}$  is not possible due to computational issues related with the network  
 338 size  $N$ , as introduced in Section 4. Alternatively, the rank of  $\mathbf{S}$  is used, providing a maximum number of isolable faults  
 339 approximation considering all the sensors available, that is 2828. Since this value is close to  $N$ , it may be considered  
 340 a feasible approximation of the maximum number of isolable faults. Also, the maximum number of isolable faults  
 341 considering all the sensors available and  $d_{\text{cluster}}$  ( $\zeta_{\text{best}}$ ) is 2824 (the 99.9 % of  $N = 2828$  nodes forming the network).  
 342 It may be observed how the relaxation by  $d_{\text{cluster}}$  does not either have much impact in this DMA when having all the

Table 2: Isolation assessment results, Canyars DMA

Number of sensors	2	3	4
$\zeta_{\text{opt}}$	267	388	388
% of $N$	38	56	56
% of $\zeta_{\text{best}}$	67	97	97
% of $\zeta_{\text{best}_0}$	67	97	97
$\zeta_{\text{opt}_0}$	116	242	245
$\rho$	0.7375	0.7342	0.7321

Table 3: Isolation results, Castelldefels Platja DMA

Number of sensors	4	5	6
$\zeta_{\text{opt}}$	2649	2665	2665
% of $N$	93.67	94.24	94.24
% of $\zeta_{\text{best}}$	93.8	94.37	94.37
% of rank $\mathbf{S}$	93.67	94.24	94.24
$\zeta_{\text{opt}_0}$	902	982	1067
$\rho$	0.5116	0.5086	0.5071

sensors available (i.e.  $\phi_{\text{best}} \cong 1$ ), but it does as in Canyars DMA when limited number of sensors are available (see Table 3) e.g. for four sensors, with  $\zeta_{\text{opt}} = 2649$  and  $\zeta_{\text{opt}_0} = 902$ ,  $\delta = 62\%$  extra coverage over  $\zeta_{\text{best}}$  is achieved when geographically relaxing the assessment. According to the specified  $d_{\text{cluster}} = 200$  m and  $d_{\text{max}} = 7222$  m, the cost function parameters have been chosen of  $d_c = 6.41$  and  $d_f = 0.46$ , respectively.

Isolation assessment results concerning sensor distribution for different number of sensors (from four to six) are detailed in Table 3. It may be seen how, for five and six sensors, the number of isolable faults for the optimal sensor set ( $\zeta_{\text{opt}}$ ) equals 2665, so according to the criterion presented here, no advantage is obtained from the usage of this extra sensor. Hence, the number of suggested sensors for this network is five (Figure 9b), achieving a theoretical coverage of the 94.24 % of the total possible faults.

## 6. Conclusions

In this paper, a new sensor placement and leak location assessment methodologies have been proposed, in order to improve the performance of leak location in water distribution networks, which may have severe impact on maintenance costs and performance of the water distribution along DMAs. Common problems arising on the leak location in large real water networks can be addressed at the sensor placement stage, e.g. leak discriminability and large location areas, when taking into account real world leak diagnosis trade-offs related with geographic location precision. Hence, a general method of sensor placement is proposed, taking into account these trade-offs by clustering similar leaks geographically, within an acceptable location area from the application point of view. The proposed method achieved promising leak location results —evaluated by an also proposed general assessment method for leak diagnosis in water distribution systems— in a small illustrative DMA in Hanoi and two larger DMAs in the Barcelona urban area. These results motivate the use of the proposed methodology in the actual and similar water networks. Further work involves to consider the number of sensors to install as part of the optimisation problem, as well as to take into account the uncertainty —existing e.g. in the sensor measurements and in the demand model— in the sensor placement algorithm, in order to cope with more realistic assumptions. Also, the extension to multiple leak scenarios may be considered in future steps of this work, by e.g. developing further methods in order to expand the sensitivity matrix accordingly, taking into account that the selection of these new scenarios should be performed carefully, in order to avoid computational issues derived from handling high dimension matrices.

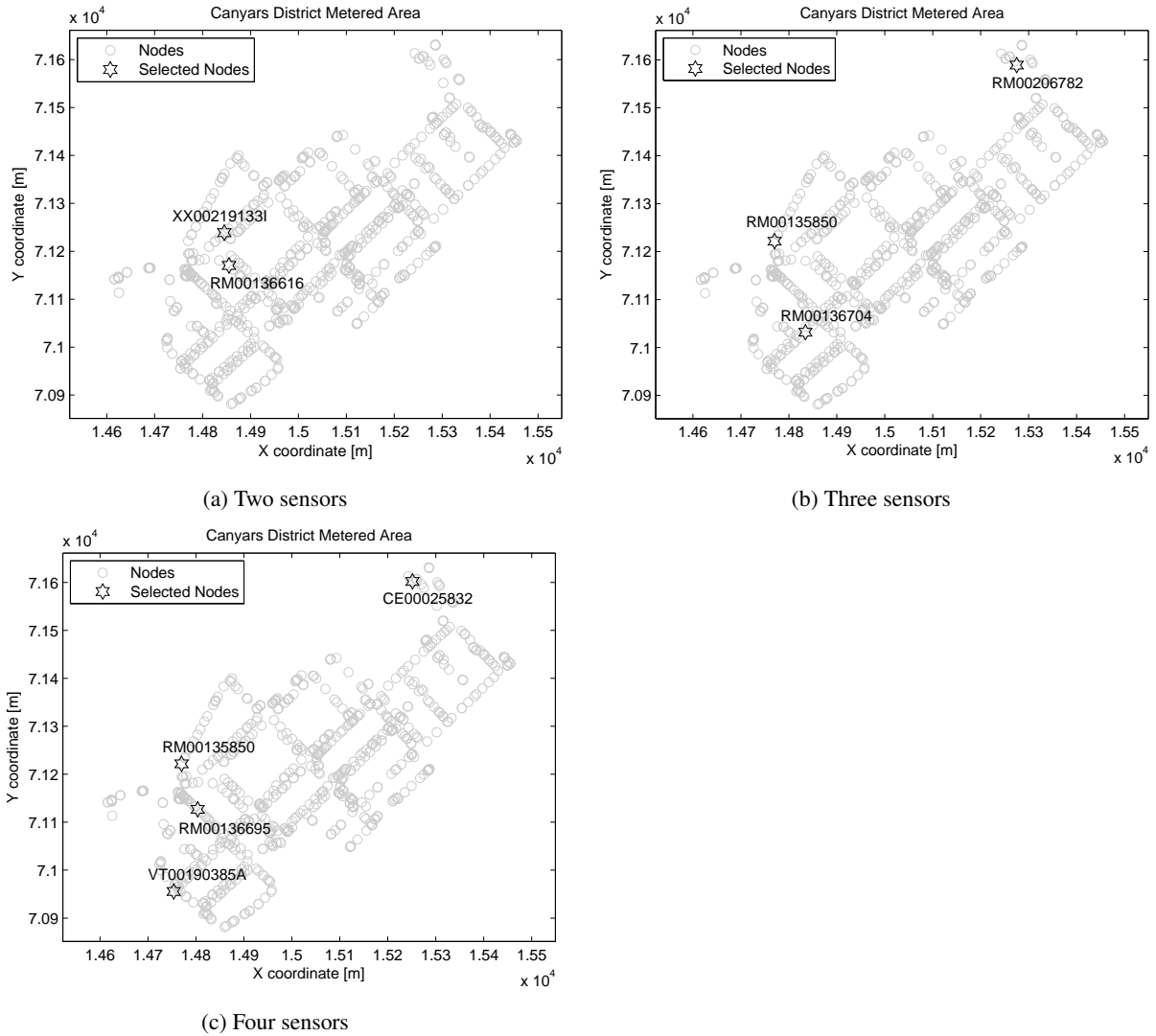


Figure 8: Sensor placement in Canyars DMA

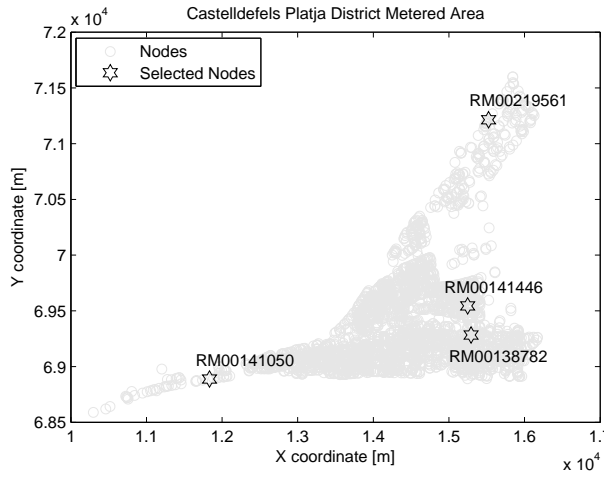
### 369 Acknowledgement

370 This work has been partially funded by the Spanish Ministry of Science and Technology through the Project  
 371 ECOICIS (Ref. DPI2013-48243-C2-1-R) and Project HARCRICS (Ref. DPI2014-58104-R), and by EFFINET grant  
 372 FP7-ICT-2012-318556 of the European Commission. The authors also wish to thank the support received by the  
 373 Water Technological Center (CETAQUA) of the company managing the Barcelona water network (AGBAR).

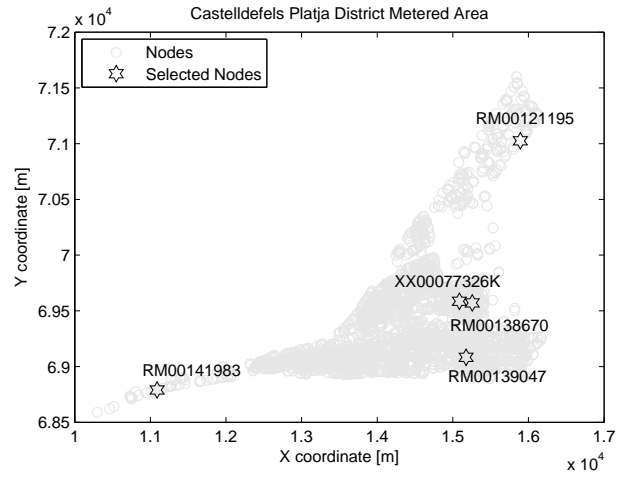
### 374 References

- 375 [1] Y. Khulief, A. Khalifa, R. Mansour, M. Habib, Acoustic detection of leaks in water pipelines using measurements inside pipe, *Journal of*  
 376 *Pipeline Systems Engineering and Practice* 3 (2) (2012) 47–54.
- 377 [2] M. Lambert, A. Simpson, J. Vitkovsky, X.-J. Wang, P. Lee, A review of leading-edge leak detection techniques for water distribution systems,  
 378 in: *20th AWA Convention*, Perth, Australia, 2003.
- 379 [3] R. Puust, Z. Kapelan, D. A. Savic, T. Koppel, A review of methods for leakage management in pipe networks, *Urban Water Journal* 7 (1)  
 380 (2010) 25–45.

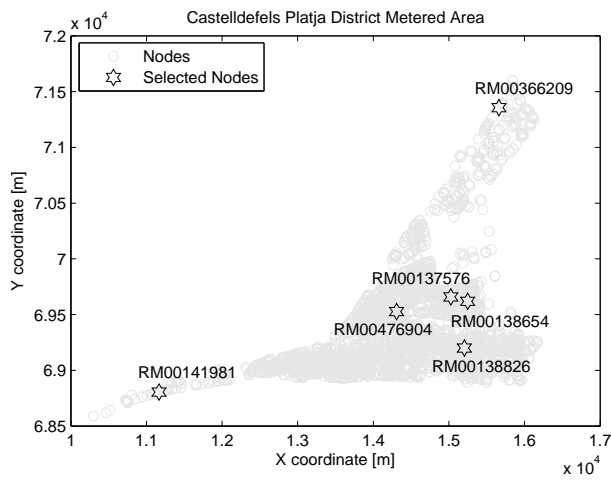




(a) Four sensors



(b) Five sensors



(c) Six sensors

Figure 9: Sensor placement in Castelldefels Platja DMA

- 381 [4] A. Lambert, What do we know about pressure leakage relationships in distribution systems?, in: IWA Conference System Approach to  
 382 leakage control and water distribution system management, no. May, Brno, Czech Republic, 2000, pp. 1–9.
- 383 [5] J. Thornton, A. Lambert, Progress in practical prediction of pressure: leakage, pressure: burst frequency and pressure: consumption relation-  
 384 ships, in: Leakage Conference Proceedings, Halifax, Canada, 2005, pp. 1–10.
- 385 [6] A. F. Colombo, P. Lee, B. W. Karney, A selective literature review of transient-based leak detection methods, *Journal of Hydro-environment*  
 386 *Research* (2009) 212–227.
- 387 [7] R. S. Pudar, J. A. Liggett, Leaks in pipe networks, *Journal of Hydraulic Engineering* 118 (7) (1992) 1031–1046.
- 388 [8] R. Pérez, V. Puig, J. Pascual, J. Quevedo, E. Landeros, A. Peralta, Methodology for leakage isolation using pressure sensitivity analysis in  
 389 water distribution networks, *Control Engineering Practice* 19 (10) (2011) 1157 – 1167. doi:10.1016/j.conengprac.2011.06.004.
- 390 [9] M. V. Casillas, L. Garza-Castañón, V. Puig, Model-based leak detection and location in water distribution networks considering an extended-  
 391 horizon analysis of pressure sensitivities, *Journal of Hydroinformatics* 16 (2014) 649–670.
- 392 [10] R. Pérez, M. A. Cugueró, J. Cugueró, G. Sanz, Accuracy assessment of leak localisation method depending on available measurements,  
 393 *Procedia Engineering* 70 (2014) 1304–1313. doi:10.1016/j.proeng.2014.02.144.
- 394 [11] A. Yassine, S. Ploix, J. M. Flaus, A method for sensor placement taking into account diagnosability criteria, *International Journal of Applied*  
 395 *Mathematics and Computer Science* 18 (4) (2008) 497–512. doi:10.2478/v10006-008-0044-5.
- 396 [12] A. Rosich, R. Sarrate, F. Nejari, Optimal sensor placement for FDI using binary integer linear programming, in: 20th International Workshop  
 397 on Principles of Diagnosis, DX09, 2009, pp. 235–242.
- 398 [13] A. Krause, J. Leskovec, C. Guestrin, J. Vanbriesen, C. Faloutsos, Efficient sensor placement optimization for securing large water distribution  
 399 networks, *Journal of Water Resources Planning and Management* 134 (6) (2008) 516–526.
- 400 [14] M. Aral, J. Guan, M. Maslia, Optimal design of sensor placement in water distribution networks, *Journal of Water Resources Planning and*  
 401 *Management* 136 (1) (2010) 5–18.
- 402 [15] R. Sarrate, F. Nejari, A. Rosich, Sensor placement for fault diagnosis performance maximization in distribution networks, in: *Control &*  
 403 *Automation (MED)*, 2012 20th Mediterranean Conference on, 2012, pp. 110–115.
- 404 [16] S. Christodoulou, A. Gagatsis, A. Xanthos, S. Kranioti, A. Agathokleous, M. Fragiadakis, Entropy-based sensor placement optimization for  
 405 waterloss detection in water distribution networks, *Water Resources Management* 27 (13) (2013) 4443–4468.
- 406 [17] M. Farley, S. Trow, *Losses in Water Distribution Networks*, IWA publishing, London, 2003.
- 407 [18] J. Quevedo, M. A. Cugueró, R. Pérez, F. Nejari, V. Puig, J. M. Mirats, Leakage location in water distribution networks based on correlation  
 408 measurement of pressure sensors, in: 8th IWA Symposium on System Analysis and Integrated Assessment (Watermatex), International Water  
 409 Association (IWA), San Sebastián, 2011, pp. 290–297.
- 410 [19] C. R. Reeves (Ed.), *Modern Heuristic Techniques for Combinatorial Problems*, McGraw Hill, UK, 1995.
- 411 [20] J. R. Koza, Survey of genetic algorithms and genetic programming, *Proceedings of 1995 WESCON Conference* (1995) 589–594.
- 412 [21] L. A. Rossman, *EPANET 2 Users Manual*, Environmental Protection Agency (EPA), U.S. (September 2000).
- 413 [22] L. Rokach, O. Maimon, Clustering methods, in: *Data Mining and Knowledge Discovery Handbook*, 2005, pp. 321–352.
- 414 [23] K. Gallagher, M. Sambridge, Genetic algorithms: A powerful tool for large-scale nonlinear optimization problems, *Computers & Geosciences*  
 415 20 (7-8) (1994) 1229–1236.
- 416 [24] T. Fawcett, An introduction to ROC analysis, *Pattern Recognition Letters* 27 (8) (2006) 861–874.
- 417 [25] M. V. Casillas-Ponce, L. E. Garza-Castañón, V. Puig-Cayuela, Model-based leak detection and location in water distribution networks consid-  
 418 ering an extended-horizon analysis of pressure sensitivities, *Journal of Hydroinformatics* 16 (3) (2014) 649–670. doi:10.2166/hydro.2013.019.
- 419 [26] T. Walski, D. Chase, D. Savic, W. Grayman, S. Beckwith, E. Koelle, *Advanced Water Distribution Modeling and Management*, Haestad  
 420 Press, 2003.